

# Highly Sensitive, Patternable Organic Films at the Nanoscale Made by Bottom-Up Assembly

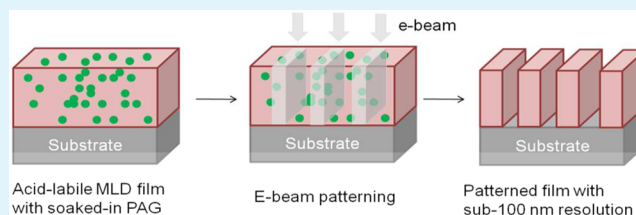
Han Zhou,<sup>†</sup> James M. Blackwell,<sup>‡</sup> Han-Bo-Ram Lee,<sup>§</sup> and Stacey F. Bent<sup>\*,§</sup>

<sup>†</sup>Department of Chemistry and <sup>§</sup>Department of Chemical Engineering, Stanford University, 381 North-South Axis, Stanford, California 94305, United States

<sup>‡</sup>Intel Corporation, Hillsboro, Oregon 97124, United States

**ABSTRACT:** Nanoscale patterning of organic thin films is of great interest for next-generation technologies. To keep pace with the demands of state-of-the-art lithography, both the sensitivity and resolution of the patternable thin films need to be improved. Here we report a highly sensitive polyurea film grown by bottom-up assembly via the molecular layer deposition (MLD) technique, which allows for high-resolution patterning at the nanoscale. The MLD process used in this work provides an exceptionally high degree of control over the film thickness and composition and also offers high coating conformality. The polyurea film was formed by urea coupling reactions between 1,4-diisocyanatobutane and 2,2'-(propane-2,2-diylidioxo)diethanamine precursors and deposited in a layer-by-layer fashion. Acid-labile ketal groups were incorporated into the backbone of the polymer chains to ensure chemically amplified cleaving reactions when combined with photoacid, which was generated by electron-beam activation of triphenylsulfonium triflate soaked into the polyurea film. With electron-beam lithography, sub-100  $\mu\text{C}/\text{cm}^2$  sensitivity and sub-100 nm resolution were demonstrated using this new bottom-up assembly approach to resist fabrication.

**KEYWORDS:** molecular layer deposition, polyurea film, patterning, sensitivity, resolution



## INTRODUCTION

The ability to make patterned organic films is an enabling factor for a variety of key technologies in use today, including integrated circuits, microfluidic devices, and bioselective surfaces.<sup>1,2</sup> Developing the means to extend the existing patterning capabilities to ever smaller size scales will be critical for next-generation technologies. As a consequence, the past decades have seen significant effort expended on advancing both the materials and techniques for nanoscale patterning. Both “bottom-up” and “top-down” methods have been developed for the fabrication of patterned organic films. Bottom-up methods rely on the presence of an initial surface pattern, typically generated by techniques such as photolithography, electron-beam lithography, nanoimprint or micro-contact printing, which is then propagated upward into an organic film. For example, surface-initiated polymerization (SIP) of monomers has been carried out on an initiator layer to make brushlike polymers from the bottom up.<sup>3,4</sup> Despite the promise of the bottom-up patterning approach, there are several disadvantages, including the necessity of many processing steps and concomitant contamination, that may lead to loss of pattern resolution. In addition, when the polymer chain length is close to the pattern’s feature size, lateral polymer growth can take place and impose limitations on the resolution.<sup>5</sup>

On the other hand, “top-down” patterning methods work by first forming a uniform organic film coating and then making patterns using various lithographic techniques. While top-down

approaches have been in commercial use for decades, one of the growing challenges with the method is making responsive organic films with sufficient sensitivity and homogeneity to achieve fine patterns. With the development of double-patterning lithography, 32 nm half-pitch resolution has been achieved in top-down processing but at the cost of reduced throughput.<sup>6</sup> Interestingly, some recent efforts have explored the use of bottom-up methods to make the lithographically responsive organic films, which are then combined with top-down lithography. The motivation for this approach is the promise of a higher degree of control in the resist layer combined with the potential for higher resolution. For example, Rastogi et al. reported a method in which polymer brushes consisting of an electron-beam sensitive compound, e.g., poly(methyl methacrylate) (PMMA), were first grown on blanket substrates by surface-initiated atom-transfer radical polymerization (ATRP), and then exposed to an electron beam to carry out chain scission and thus achieve direct nanoscale patterns.<sup>7</sup> However, similar to bulk PMMA, which is a widely known nonchemically amplified photoresist material, these electron-beam-sensitive polymer brushes did not have high sensitivity and usually required doses of more than 100  $\mu\text{C}/\text{cm}^2$ , which imposed a limitation on the throughput of this direct patterning technique. Jeon et al. developed a similar

**Received:** January 22, 2013

**Accepted:** April 1, 2013

**Published:** April 17, 2013

approach to achieve 80 nm features by two-photon laser ablation of the surface poly(ethylene glycol) methacrylate layer grown by ATRP.<sup>8</sup> Again, the energy density needed was on the order of joules per square centimeter, a value too high for modern lithographic requirements. In addition to the low sensitivity, most of the surface organic layers grown to date using bottom-up methods such as SIP were prepared in solution, an environment that may not provide a sufficiently high level of control over the film thickness, conformality, or chemical composition.

Here we show how these limitations can be overcome by a bottom-up, rational-design method for fabricating chemically amplified, nanoscale organic resists with molecular-level control. Specifically, we report a novel method to make patterned organic films with high resolution (sub-50 nm) and excellent sensitivity (sub-100  $\mu\text{C}/\text{cm}^2$ ) by direct electron-beam patterning of an intrinsically chemically amplified organic film deposited using molecular layer deposition (MLD).

MLD is an emerging technique for growing organic thin films. It deposits films in a layer-by-layer fashion by utilizing a series of self-limiting reactions of multifunctional organic precursor molecules.<sup>9,10</sup> Using this technique, polyamide, polyimide, and polyurea films have been grown based on amide,<sup>11–14</sup> imide,<sup>15–17</sup> urea,<sup>18–20</sup> and thiourea<sup>21</sup> coupling chemistries, respectively. MLD offers several advantages over conventional solution-phased polymerization methods. First, the film thickness can be controlled at the angstrom level because of the self-limiting nature of the linking reactions used in MLD. Second, MLD can provide highly conformal coatings even on substrates with high-aspect-ratio patterns. Third, the film composition can be precisely tuned by introducing precursor molecules with desired functionality embedded into the backbone at a particular cycle during the deposition. In this way, the concentration and position of the desired functionality can be readily controlled. These advantages can be valuable for subsequent utilization of the organic films for patterning.

In previous work, we carried out initial tests of this idea by growing an ultrathin polyurea film by MLD using 1,4-phenylenediisocyanate (PDIC) and 2,2'-(propane-2,2-diylidioxy)diethanamine (PDDE) designed as a chemically amplified resist.<sup>22</sup> Chemical amplification is important because it can greatly enhance the patterning sensitivity of the organic film and thus the throughput of the patterning process. Investigation into the patterning of this MLD film showed that a resolution of at least 4  $\mu\text{m}$  could be achieved.<sup>22</sup> However, the patterning in that study was limited because the MLD film cross-linked under the electron-beam irradiation that was used for high-resolution patterning. In the present work, we have developed an improved approach that allows us to achieve patterning of the film with a resolution of sub-50 nm and a sensitivity of sub-100  $\mu\text{C}/\text{cm}^2$  under 100 kV electron-beam irradiation. The ultrathin organic film that we deposit by MLD is directly patternable and chemically amplified at thicknesses of only 30 nm. This work introduces a powerful yet simple method for patterning in nanoscale organic films that may enable future nanotechnologies. It provides not only a novel route to make patterns on organic films but also the potential to rationally design and deposit various functionalities and ultimately achieve the desired properties of the patterned polymer layer.

## EXPERIMENTAL METHODS

MLD films were deposited in a hot-wall flow reactor pumped by a Leybold Trivac rotary vane pump with a base pressure below 1 mTorr. The reactor was heated by an external heating tape that was controlled by a variable transformer. MLD precursors and nitrogen purge gas were introduced into the reactor using Swagelok ALD valves, which were controlled by a *LabVIEW* program.

(3-Aminopropyl)triethoxysilane (APTES), 1,4-diisocyanatobutane (DICB), triphenylsulfonium triflate (TPSOTf), and propylene glycol methyl ether acetate (PGMEA) were purchased from Sigma-Aldrich and used as received. A tetramethylammonium hydroxide (TMAH) aqueous solution (25 wt %) was also purchased from Sigma-Aldrich and diluted in  $\text{H}_2\text{O}$  to the desired concentrations. 2,2'-(Propane-2,2-diylidioxy)diethanamine (PDDE) was synthesized using the method reported in the literature.<sup>23</sup> Films were deposited on silicon (100) wafers with a 4-nm-thick thermal oxide.

Prior to MLD cycles, silicon wafers were cleaned with a piranha solution followed by an APTES surface functionalization using a process reported in the literature<sup>24</sup> and described in detail in our previous study.<sup>19</sup> Each complete binary MLD cycle contains a 6-min DICB dose, followed by a 3-min nitrogen gas purge, and then a 5-min PDDE dose, followed by a 4-min nitrogen gas purge. The dosing procedure for DICB was to keep the valve to the sample vial open for 2.5 min and then allow DICB to remain in the reactor for the remaining 3.5 min of the dose, and that for PDDE was to keep the valve to the sample vial open for the entire 5-min dosing time. MLD was performed with the reactor, substrate, and the two precursors all at room temperature. After MLD, samples were taken out of the reactor for ex situ analysis and characterization.

The film growth starts from an amine-terminated surface formed by APTES exposure to the  $\text{SiO}_2$ -coated substrate, and the subsequent MLD scheme is shown in Figure 1. This scheme is related to one that

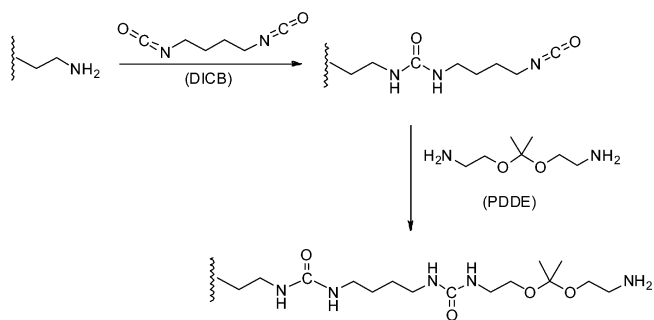


**Figure 1.** MLD scheme for growth of a patternable polyurea film using DICB and PDDE.

we reported previously,<sup>22</sup> a key difference is replacement of the aromatic phenylene group in the backbone of the PDIC precursor by an aliphatic butylene group using the DICB precursor. This change was carried out to eliminate the aromatic components in the MLD film, which may be a source of cross-linking under electron-beam exposure and may adversely affect the sensitivity of the polymer film.<sup>25</sup> The piranha-cleaned  $\text{SiO}_2$  surface was first coated by an APTES self-assembled monolayer (SAM), leaving the surface terminated with amine groups after the silanization reaction. Following the formation of the SAM priming layer, the DICB precursor was introduced into the reactor and attached to the surface via a urea coupling reaction between the amine and isocyanate groups. A PDDE dose was subsequently introduced into the reactor and reacted with surface isocyanate groups via urea coupling. A DICB dose and a PDDE dose formed a complete MLD cycle, which was repeated until the desired film thickness was achieved.

Following deposition of the acid-labile DICB/PDDE polyurea MLD film, another important component, the photoacid generator (PAG), was incorporated into the MLD film to achieve a directly patternable film. Incorporation of the TPSOTf PAG was done by immersing the

MLD films into a 0.015 M saturated solution of TPSOTf in PGMEA for 12 h on a 65 °C hot plate; the PGMEA solvent was blown dry with compressed air after the immersion. No residual TPSOTf crystallites were observed on the sample surface after drying the PGMEA solvent, and no postsoaking rinse was used. Because a homogeneous TPSOTf solution and a long soaking time were employed, a relatively uniform lateral distribution of the TPSOTf PAG can be expected. Our previous X-ray photoelectron spectroscopy (XPS) study on a PAG-soaked MLD film shows that film composition is consistent at different locations of the sample. As shown in our previous report,<sup>22</sup> Fourier transform infrared (FTIR) and XPS measurements confirmed the successful incorporation of the TPSOTf PAG into the MLD film, although it is difficult to quantify the amount of soaked-in PAG. We have also noticed that, according to XPS depth-profiling measurements, the film surface has more PAG incorporation than the bottom of the film. TPSOTf PAG incorporation comprised the last step of the formation of a directly patternable film. Electron-beam patterning was performed at the Molecular Foundry at Lawrence Berkeley National Laboratory using a Vistec VB300UHR EWF electron-beam lithography system. A beam voltage of 100 kV was used to write the patterns. After electron-beam exposure, the MLD films underwent postexposure bake (PEB) on a hot plate for 90 s and then were developed in a 0.26 M aqueous TMAH solution for 45 s, rinsed with deionized (DI) H<sub>2</sub>O, and finally blown dry using compressed nitrogen. The lowest dose tested was 25  $\mu\text{C}/\text{cm}^2$  because inaccuracy starts to become significant at electron-beam doses below this value.

Film thicknesses were measured using a Gaertner Scientific Corp. L116C He–Ne laser ellipsometer with 632.8 nm light. At least three different locations on each sample were measured so as to test the film uniformity across it. Because the refractive indices of the SiO<sub>2</sub> and organic film are very close, a refractive index of 1.46 was used for both materials.<sup>26–28</sup> The thickness of the organic film deposited on the SiO<sub>2</sub> layer was determined by subtracting the baseline SiO<sub>2</sub> thickness of piranha-cleaned silicon samples from the subsequent total film thickness values. FTIR spectroscopy measurements were performed on a Thermo Nicolet 6700 FTIR spectrometer using a MCT-A detector in the transmission mode. Spectra were taken with 200 scans at 4  $\text{cm}^{-1}$  resolution. Piranha-cleaned silicon samples were used as a background reference. XPS was performed on a Physical Electronics, Inc., 5000 Versaprobe spectrometer using Al K $\alpha$  radiation (1486.6 eV) as the excitation source. Survey scans were performed to measure the elemental composition of each sample using an energy step of 1 eV. Atomic compositions were calculated by determining the peak areas, and peaks were fit using Gaussian profiles with a Shirley background. Images of the patterns were taken by an FEI Magellan 400 XHR scanning electron microscope with a secondary electron detector as well as a Park XE-70 atomic force microscope. For cross-sectional scanning electron microscopy (SEM) images, samples were fractured under cryogenic conditions to prevent deformation of the MLD film. Atomic force microscopy (AFM) was carried out using high-aspect-ratio silicon nitride tips, with a radius of curvature less than 15 nm, in a tapping mode.

## RESULTS AND DISCUSSION

The organic resist film reported here is formed via a urea coupling reaction between a diisocyanate precursor, DICB, and a diamine precursor, PDDE, with the acid-labile ketal group embedded in the backbone of the PDDE (Figure 1). During the MLD process, layer-by-layer film growth is achieved by alternating doses of these two precursors. The growth of the film was characterized using a combination of spectroscopic and microscopic methods. The polyurea film thicknesses were measured after various numbers of MLD cycles, as shown in Figure 2a. The film thickness is a linear function of the number of MLD cycles. Three separate experimental series measuring the thickness versus the number of MLD cycles were performed to test the repeatability of the MLD process, and an average film growth rate of  $1.9 \pm 0.2 \text{ \AA}/\text{cycle}$  was found.

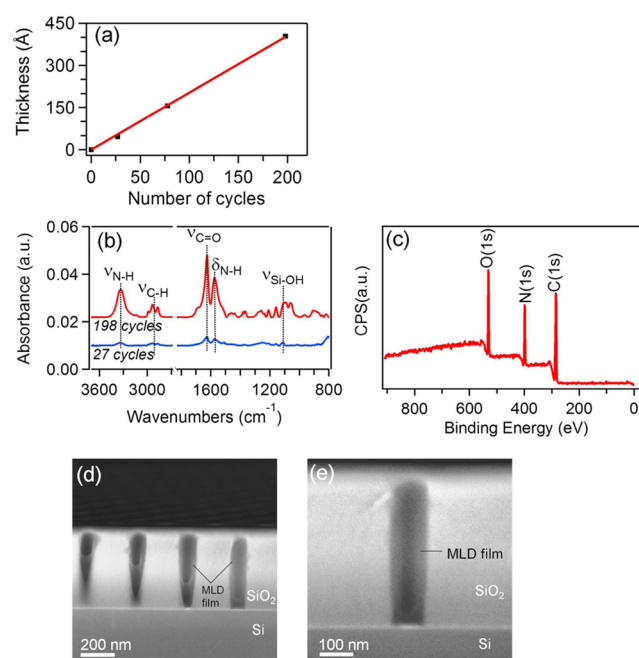


**Figure 2.** (a) Plot of the polyurea film thickness as a function of the number of MLD cycles. (b) FTIR spectra of polyurea films after 27 and 198 MLD cycles. (c) XPS spectrum of a 198-cycle polyurea film. (d and e) Cross-sectional SEM images of vias coated with an MLD film.

This growth rate is much lower than that of its aromatic analogue film grown using PDIC/PDDE precursors,<sup>22</sup> which may be explained by the difference in the rigidities of the monomer chains. For the aliphatic polyurea film formed by DICB/PDDE, the polymer chains are more flexible than those in the aromatic film formed by PDIC/PDDE, which may lead to a higher degree of tilting toward the surface, in turn presenting as a lower growth rate in angstroms per cycle.

FTIR spectra were taken to investigate the chemical bonding of the polyurea films after different numbers of MLD cycles, as shown in Figure 2b. All IR peak intensities increased with the cycle numbers with increasing film thickness. Characteristic peaks of urea linkage were observed in the films at 1625.6 and 1575.3  $\text{cm}^{-1}$  and assigned to the amide I ( $\nu_{\text{C=O}}$ ) and amide II ( $\delta_{\text{N-H}}$ ) modes, respectively.<sup>29</sup> Other important peaks, such as the  $\nu_{\text{N-H}}$  mode at 3333.9  $\text{cm}^{-1}$  and  $\nu_{\text{C-H}}$  modes at 2989.0, 2937.9, and 2869.8  $\text{cm}^{-1}$ , were also observed as expected. The presence of these IR absorptions confirmed that the deposited film was covalently propagated via urea coupling reactions rather than condensation of precursor molecules.

Another important characteristic of the polyurea film is its chemical composition, which was investigated by XPS measurement on a sample after 198 MLD cycles, as shown in Figure 2c. The experimental atomic ratio of C/N/O calculated from the XPS spectrum is  $3.09 \pm 0.08/0.97 \pm 0.04/1$ , whereas the ideal ratio is 3.25/1/1. The good agreement between the experimental and ideal ratios indicates that the polyurea films were deposited with stoichiometric composition through urea linkages.

MLD, as an analogue of atomic layer deposition (ALD), can provide a highly conformal coating of a structured substrate.<sup>21</sup> To examine the conformality of the MLD films, a SiO<sub>2</sub> substrate with vias that are 90 nm in diameter and 450 nm in depth was used for film growth. After deposition of a 25 nm

MLD film, the sample was cleaved across the vias, and cross-sectional SEM images were taken. The results, shown in Figure 2d,e, indicate that the vias are conformally coated. The apparent variation in the depths of adjacent vias in Figure 2d resulted from slightly off-axis sample fracturing. Although the SEM image does not exhibit optimal contrast and sharpness, it is still indicative that the MLD coating is quite conformal. Moreover, Figure 2e shows the image of a well-cut via, and it is evident that the MLD coating is uniform throughout the via. A similar demonstration of the conformality in MLD was previously reported by our group,<sup>21</sup> wherein a 14 nm polythiourea MLD film was deposited on silica nanoparticles and shown by transmission electron microscopy imaging to be highly conformal. The via coating imaged in Figure 2d,e is thus an additional confirmation that the MLD technique can provide excellent conformality.

These MLD films were rationally designed to incorporate the components of a chemically amplified resist. In other words, our ketal-embedded polyurea MLD films allow chemically amplified cleavage of the polymer chains to take place through catalytic acid generation, in which photoacid generated by the TPSOTf PAG can trigger more than one cleaving reaction across the polymer backbone. This amplification can greatly increase the sensitivity of the resist. Sensitivity, which characterizes the material's ability to utilize the incident photon or electron beam, is one of the key parameters describing the performance of a patternable material.

To test the resist sensitivity of the MLD materials, electron-beam patterning was carried out on the polyurea films, followed by PEB and development. Two different PEB temperatures, 70 and 75 °C, were examined, and the contrast curves plotting the normalized film thickness against the corresponding electron-beam dose are shown in Figure 3a. These PEB temperatures are expected to be well below the glass transition temperature ( $T_g$ ) of the MLD resist. Although the direct measurement of  $T_g$  of the MLD resist is difficult because the film is sitting on a substrate, a similar polyurea film formed by vapor deposition

polymerization was reported to have a  $T_g$  of 120–180 °C.<sup>30</sup> The contrast curve of 70 °C PEB is in good agreement with typical positive tone resist behavior. In addition, at 75 °C PEB, the curve shifts to lower electron-beam doses. The data clearly show that, by increasing the PEB temperature by 5 °C, the sensitivity of the polyurea film is enhanced because the minimum dose required to clear the film in the exposed region decreases from 75 to 30  $\mu\text{C}/\text{cm}^2$ . It should also be noted that good repeatability was observed for the MLD resist. For example, another MLD film that underwent 2 min of PEB at 70 °C showed a sensitivity of 72  $\mu\text{C}/\text{cm}^2$ , which is very close to the sensitivity of 75  $\mu\text{C}/\text{cm}^2$  as mentioned above. This observation of the temperature dependence is in agreement with the expected behavior of an acid-catalyzed cleaving reaction because increasing the temperature enhances the reactivity of the photoacid (i.e., the catalyst), and therefore one photoacid triggers more cleaving reactions at the ketal sites in the polymer backbone. To improve the contrast of the MLD photoresist film beyond that shown in Figure 3a, further optimization of parameters such as the PAG loading and potential addition of a base quencher needs to be performed.

Interestingly, when treated at a high PEB temperature (75 °C), the contrast curve also shows an abnormality at high dose, in which less film is removed as the dose increases for large electron-beam doses. This phenomenon can be explained by the electron-beam-induced cross-linking of the polymer chains, which hardens the polymer film and makes it less soluble in the developer. Because heat, together with electron-beam exposure, is commonly needed for the cross-linking reaction of a photoresist to proceed,<sup>31</sup> PEB at 75 °C may have increased the cross-linking efficiency, while PEB at 70 °C was not sufficient to form detectable cross-linking in the film. However, it should be noted that this degree of cross-linking is much lower than that previously reported for a PDIC/PDDE MLD film, which shows cross-linking behavior even at very low electron-beam dose likely because of the presence of aromatic rings. Moreover, when the DICB/PDDE MLD film is compared to the most widely used PMMA electron-beam resist, it is evident that the film reported here performs with greater sensitivity. Specifically, PMMA has a sensitivity of about 350  $\mu\text{C}/\text{cm}^2$  using a 50 kV electron beam,<sup>32</sup> which scales to 700  $\mu\text{C}/\text{cm}^2$  when using a 100 kV electron beam like in our study, a value much larger than the 30  $\mu\text{C}/\text{cm}^2$  reported here for the MLD film. Hence, our MLD film is highly sensitive and utilizes incident electrons much more efficiently than the commercial standard. However, compared to some other chemically amplified photoresists, e.g., the ARCH photoresist with a sensitivity of 8–16  $\mu\text{C}/\text{cm}^2$  at 50 kV, which scales to 16–32  $\mu\text{C}/\text{cm}^2$  at 100 kV,<sup>32</sup> the MLD resist film had a slightly lower sensitivity. It should be noted that many patterning processing parameters, such as the dose, PEB temperature, PEB time, developer concentration, and developing time, have not yet been optimized for the MLD film, and it is likely that such optimization can further improve the sensitivity of the MLD resists.

Besides sensitivity, another important parameter in lithographic resists is pattern resolution. Resolution measures the smallest feature size that can be achieved using the material. To test the resolution in the MLD materials, features consisting of lines and dots of various sizes were patterned on the polyurea film with a dose chosen according to the contrast curve. Parts b and c of Figure 3 show SEM images of 150 nm lines and dots, respectively, with a pitch of 300 nm. It can be seen that the

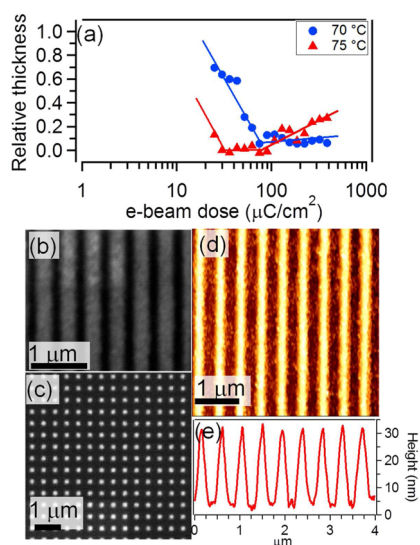


**Figure 3.** (a) Normalized film thickness as a function of the electron-beam dose at PEB temperatures of 70 and 75 °C, respectively. The lines are guides to the eye. (b–e) Features obtained on 32-nm-thick polyurea films, patterned with an electron-beam dose of 100  $\mu\text{C}/\text{cm}^2$  and PEB at 70 °C.

patterned lines using the polyurea films are highly uniform over a large spatial dimension. Figure 3d shows an AFM image of the line features in part b, and Figure 3e is the cross-sectional depth profile of part d. The trench depth is about 32 nm, which is the same as the thickness of the polyurea film used for patterning, indicating that the polyurea MLD film in the exposed region was effectively removed by the electron-beam lithographic process.

To further test the limits of resolution, the MLD resists were patterned with features at a sub-100-nm scale (Figure 4). Panels

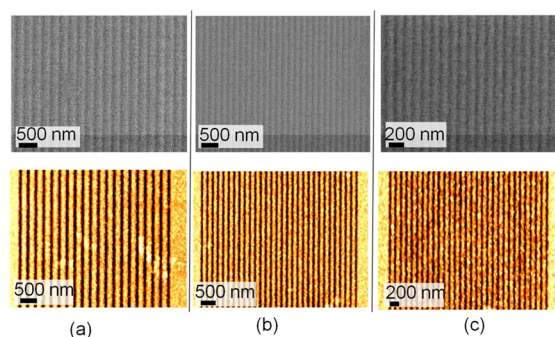


**Figure 4.** SEM (top row) and AFM (bottom row) images of line features obtained on a 21 nm polyurea film by an electron-beam exposure dose of  $48 \mu\text{C}/\text{cm}^2$  and PEB at  $70^\circ\text{C}$ : (a) 80 nm lines with a pitch size of 160 nm, or a half-pitch size of 80 nm; (b) 60 nm lines with a pitch size of 120 nm; (c) 40 nm lines with a pitch size of 80 nm.

a–c show SEM images (top) and AFM images (bottom) of 80, 60, and 40 nm half-pitch lines, respectively. Although the SEM images are not very sharp because of a charging effect of the organic films during measurement, the AFM images clearly show the high quality of the patterning results. The features are resolved with high quality with a line width as small as 40 nm, which is fine enough to be useful for a wide range of different applications. As a result, it can be concluded that the directly patternable chemically amplified polyurea MLD film has an excellent patterning performance.

## CONCLUSIONS

We have demonstrated a rationally designed, bottom-up assembled polymer film that can be patterned with excellent sensitivity and resolution by an electron beam. The polymer films were deposited using a MLD technique with highly controlled thickness and excellent conformality. The films were built via urea coupling reactions and showed stoichiometric composition. Ketal groups were incorporated into the backbone of the polymer serving as acid-labile groups that underwent cleavage when triggered by a photoacid, which was generated during electron-beam exposure of soaked-in PAG. Cleavage of the polymer film occurs by a catalytic reaction pathway; hence, it is chemically amplified and ensures a high patterning sensitivity. Using electron-beam lithography, line features as small as 40 nm were achieved with sub- $100 \mu\text{C}/\text{cm}^2$  exposure. The sensitivity exceeds that of the widely used electron-beam resist PMMA, as well as other resists made from bottom-up assembly. Besides the excellent sensitivity and resolution, this novel approach to make patternable polymer films provides greater simplicity and ease of fabrication than conventional top-down then bottom-up methods. Moreover, the unprecedented coating conformality of MLD may allow this method to be

applied to very fine patterning on top of prepatterned substrates.

## AUTHOR INFORMATION

### Corresponding Author

\*E-mail: sbent@stanford.edu.

### Notes

The authors declare no competing financial interest.

## ACKNOWLEDGMENTS

We acknowledge support of this work from Intel Corporation. We thank Dr. Todd Younkin for valuable discussions about this research. Portions of this work (use of the electron-beam exposure tool) were performed as a User project at the Molecular Foundry, supported by the Office of Science, Office of Basic Energy Sciences, of the U.S. Department of Energy under Contract DE-AC02-05CH11231. Scott Dhuey and Dr. Deirdre Olynick are thanked for help with electron-beam exposure.

## REFERENCES

- Geissler, M.; Xia, Y. N. *Adv. Mater.* **2004**, *16* (15), 1249–1269.
- Nie, Z. H.; Kumacheva, E. *Nat. Mater.* **2008**, *7* (4), 277–290.
- Herzer, N.; Hoepfner, S.; Schubert, U. S. *Chem. Commun.* **2010**, *46* (31), 5634–5652.
- Ducker, R.; Garcia, A.; Zhang, J. M.; Chen, T.; Zauscher, S. *Soft Matter* **2008**, *4* (9), 1774–1786.
- Patra, M.; Linse, P. *Nano Lett.* **2006**, *6* (1), 133–137.
- Lin, B. J.; Hoefflinger, B. *Nanolithography*. *Chips* 2020; Springer: Berlin, 2012; pp 175–188.
- Rastogi, A.; Paik, M. Y.; Tanaka, M.; Ober, C. K. *ACS Nano* **2010**, *4* (2), 771–780.
- Jeon, H.; Schmidt, R.; Barton, J. E.; Hwang, D. J.; Gamble, L. J.; Castner, D. G.; Grigoropoulos, C. P.; Healy, K. E. *J. Am. Chem. Soc.* **2011**, *133* (16), 6138–6141.
- Ritala, M.; Leskela, M. *Atomic Layer Deposition*. In *Handbook of Thin Film Materials*; Nalwa, H. S., Ed.; Academic Press: San Diego, CA, 2002; Vol. 1.
- George, S. M.; Yoon, B.; Dameron, A. A. *Acc. Chem. Res.* **2009**, *42* (4), 498–508.
- Kubono, A.; Yuasa, N.; Shao, H. L.; Umemoto, S.; Okui, N. *Thin Solid Films* **1996**, *289* (1–2), 107–111.
- Shao, H. I.; Umemoto, S.; Kikutani, T.; Okui, N. *Polymer* **1997**, *38* (2), 459–462.
- Du, Y.; George, S. M. *J. Phys. Chem. C* **2007**, *111* (24), 8509–8517.
- Adarnczyk, N. M.; Dameron, A. A.; George, S. M. *Langmuir* **2008**, *24* (5), 2081–2089.
- Bitzer, T.; Richardson, N. V. *Appl. Phys. Lett.* **1997**, *71* (13), 1890–1892.
- Yoshimura, T.; Tatsuura, S.; Sotoyama, W. *Appl. Phys. Lett.* **1991**, *59* (4), 482–484.
- Bitzer, T.; Richardson, N. V. *Appl. Surf. Sci.* **1999**, *144–45*, 339–343.
- Kim, A.; Filler, M. A.; Kim, S.; Bent, S. F. *J. Am. Chem. Soc.* **2005**, *127* (16), 6123–6132.
- Loscutoff, P. W.; Zhou, H.; Clendenning, S. B.; Bent, S. F. *ACS Nano* **2010**, *4* (1), 331–341.
- Usui, H. *Thin Solid Films* **2000**, *365* (1), 22–29.
- Loscutoff, P. W.; Lee, H.-B.-R.; Bent, S. F. *Chem. Mater.* **2010**, *22* (19), 5563–5569.
- Zhou, H.; Bent, S. F. *ACS Appl. Mater. Interfaces* **2011**, *3* (2), 505–511.
- Paramonov, S. E.; Bachelder, E. M.; Beaudette, T. T.; Standley, S. M.; Lee, C. C.; Dashe, J.; Frechet, J. M. J. *Bioconjugate Chem.* **2008**, *19* (4), 911–919.

- (24) Zheng, W. W.; Frank, C. W. *Langmuir* **2010**, *26* (6), 3929–3941.
- (25) Paik, M. Y.; Xu, Y. Y.; Rastogi, A.; Tanaka, M.; Yi, Y.; Ober, C. K. *Nano Lett.* **2010**, *10* (10), 3873–3879.
- (26) Vandenberg, E. T.; Bertilsson, L.; Liedberg, B.; Uvdal, K.; Erlandsson, R.; Elwing, H.; Lundstrom, I. J. *Colloid Interface Sci.* **1991**, *147* (1), 103–118.
- (27) Haller, I. *J. Am. Chem. Soc.* **1978**, *100* (26), 8050–8055.
- (28) Howarter, J. A.; Youngblood, J. P. *Langmuir* **2006**, *22* (26), 11142–11147.
- (29) Vien, D. L.; Colthup, N. B.; Fateley, W. G.; Grasselli, J. G. *The Handbook of Infrared and Raman Characteristic Frequencies of Organic Molecules*; Academic Press: London, 1991.
- (30) Takahashi, Y.; Iijima, M.; Fukada, E. *Jpn. J. Appl. Phys., Part 2* **1989**, *28* (12), L2245–L2247.
- (31) Nordquist, K. J.; Resnick, D. J.; Ainley, E. S. *J. Vac. Sci. Technol., B* **1998**, *16* (6), 3289–3293.
- (32) Rai-Choudhury, P. *Handbook of microlithography, micromachining, and microfabrication*; SPIE Optical Engineering Press: Bellingham, WA, 1997.